

# Supporting Information for

## Switching the Surface Homochiral Assembly by Surface

### Host-Guest Chemistry

Shu-Ying Li,<sup>a,b</sup> Ting Chen,<sup>a</sup> Jie-Yu Yue,<sup>a,b</sup> Dong Wang,<sup>\*a,b</sup> and Li-Jun Wan<sup>\*a</sup>

<sup>a</sup> Key Laboratory of Molecular Nanostructure and Nanotechnology, Institute of Chemistry,  
Chinese Academy of Sciences (CAS), Beijing 100190, P.R. China

<sup>b</sup> University of Chinese Academy of Sciences, Beijing 100049, P.R.China.

#### Contents:

1. Experimental materials and methods
2. STM image of sunflower structure I
3. STM images of the enantiomeric assemblies at the (*R*)-2-nonanol/HOPG interface
4. Majority-rules principle at the 2-nonanol/HOPG interface when (*R*)-2-nonanol is excess
5. Molecular models for chiral assemblies preferred by (*R*)-2-nonanol
6. Molecular mechanistic simulations of the energies of the enantiomeric patterns containing 2-nonanol.
7. Molecular mechanistic simulations for the emergence of adaptive reorganization.

## 1. Experimental materials and methods

**Experimental details.** BIC derivatives were synthesized as described in a previous report<sup>1</sup>. Prior to imaging, the compounds (BIC derivatives or coronene) were dissolved in 2-nonanol at a concentration of  $2 \times 10^{-4}$  M. Chiral 2-nonanol and coronene were purchased from sigma-aldrich with purity of 99%. The STM tips were mechanically cut from Pt/Ir wire (90/10). All experiments were performed at room temperature using PicoSPM (Agilent Technologies) in constant-current mode. All STM images were shown without any modification.

Two sample prepared methods were employed to investigate the host–guest systems: 1) The solution of BIC derivatives was first applied onto the surface to confirm the honeycomb structure, and then a drop of the solution of the guest coronene molecules was added to the sample. 2) A mixed solution of the host (BIC derivatives) and guest (coronene) molecules was deposited to the substrate. Experimental results indicate that the methods of sample preparation have no effect on the resulting supramolecular assembly.

**Statistical methods.** For each sample, the distributions of the enantiomorphs on surface were recorded based on more than 25 large-scale STM images ( $100 \times 100$  nm<sup>2</sup>) obtained at different locations. Note that the organizational chirality given in this paper is an average value of several investigated samples.

**Molecular mechanistic simulations.** MM simulations were carried out with the molecular package TINKER using the MMFF force field<sup>2-4</sup>. 2D packing models of BIC were built according to the STM images. One hexagonal honeycomb network or four adjacent sunflower structures are used as the initial structure models. The BIC monolayers are placed 0.35 nm above the upper layer of a two-layer sheet of graphene keeping the alkyl chains in BIC parallel to the directions of graphite symmetry axes. During optimization, the graphite was frozen. As processed in previous literature<sup>5</sup>, the calculated results from MM simulations are divided by the area possessed by the hexagonal structure. Thus, the energy data provided in the text indicate the packing energy density in

different networks.

## 2. STM image of sunflower structure I

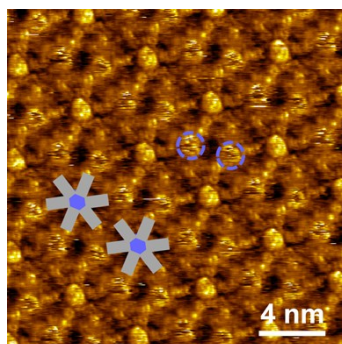


**Fig. S1** STM image of BIC-C8 at the (*S*)-2-nonanol/HOPG interface. The backbones in BIC are indicated by gray columns. Coronene surrounded by six BIC molecules is represented by blue dot. The blue dashed circles indicate the additional co-adsorbed coronene in the assembly.

## 3. STM images of the enantiomeric assemblies at the (*R*)-2-nonanol/HOPG interface

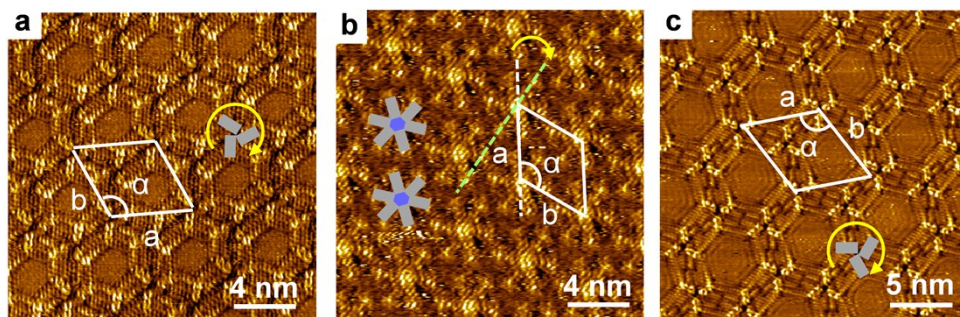


**Fig. S2** (a) The homochiral CW honeycomb network of BIC-C8 in the absence of guest coronene ( $I = 0.9 \text{ nA}$ ,  $V_{\text{bias}} = 0.900\text{V}$ ). (b) The homochiral CW sunflower structure I of BIC-C8 in the presence of guest coronene ( $I = 0.4 \text{ nA}$ ,  $V_{\text{bias}} = 0.900\text{V}$ ). The white and green dashed lines indicate the direction of the unit cell direction  $a$  and the axis of BIC molecule, respectively. (c) The homochiral CW honeycomb network of BIC-C16 in the absence of guest coronene ( $I = 1.2 \text{ nA}$ ,  $V_{\text{bias}} = 0.900\text{V}$ ). The backbones in BIC molecules are indicated by gray columns to identify chirality. The guest coronene is represented by blue dot.

#### 4. Majority-rules principle at the 2-nonanol/HOPG interface when (*R*)-2-nonanol is excess

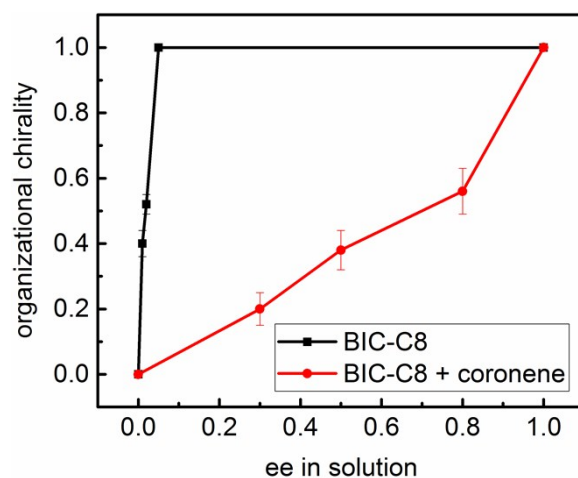


**Fig. S3** The ee in solution is defined as  $ee = (R-S)/(R+S)$ , in which *R* and *S* represent the amount of (*R*)-2-nonanol and (*S*)-2-nonanol in solution, respectively. For the organizational chirality, excess of one enantiomeric pattern is calculated according to  $\Delta N = (N_2 - N_1)/(N_1 + N_2)$ . The number of CCW or CW domains for one sample was summed up together and labeled as  $N_1$  and  $N_2$ , respectively.

#### 5. Molecular models for chiral assemblies preferred by (*R*)-2-nonanol

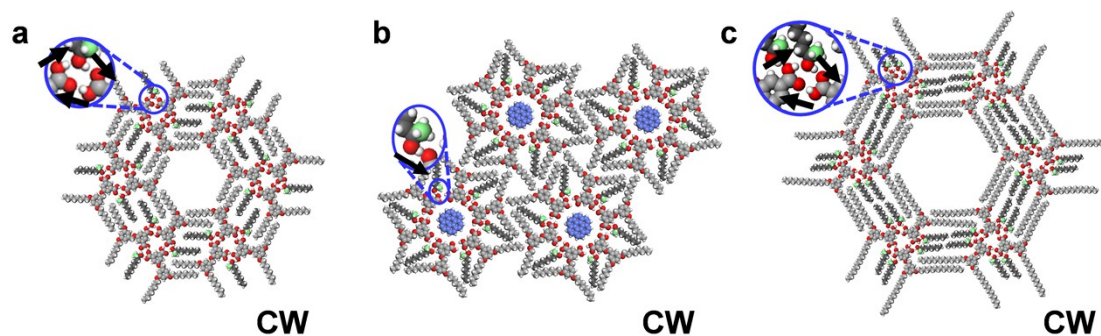


**Fig. S4** Molecular models of the enantiomeric motifs preferred by (*R*)-2-nonanol. The inset enlarges the directional CW hydrogen bonds in corresponding structure. The black arrows point to the direction of the hydrogen bond O-H...O formed by hydroxyl group in 2-nonanol and carboxylic acid group in BIC. (a) CW honeycomb structure composed of BIC-C8 and (*R*)-2-nonanol. (b) CW sunflower structure I composed of BIC-C8, (*R*)-2-nonanol and coronene. (c) CW honeycomb structure composed of BIC-C16 and (*R*)-2-nonanol. For clarity, the guest coronene and the co-adsorbed solvent 2-nonanol are colored blue and dark gray, respectively. Methyl group at the stereogenic center in 2-nonanol is painted green.

## 6. Molecular mechanistic simulations of the energies of the enantiomeric patterns containing 2-nonanol.

**Table S1.** Simulated energies in CW and CCW assemblies composed of *S*-2-nonanol. The simulated results indicate the energies per unit area and are presented in kcal·mol<sup>-1</sup>·nm<sup>-2</sup>.<sup>[a]</sup> □

Adsorption energy	$E_{CCW}$	$E_{CW}$	$E_{CW-CCW}$
Honeycomb Structure	-28.55	-25.19	3.36
Sunflower Structure I	-30.60	-29.56	1.04

[a]  $E_{CW-CCW}$  is the difference in adsorption energy between CW and CCW patterns.

## 7. Molecular mechanistic simulations for the emergence of adaptive reorganization.

We also comment on the emergence of the structural transition from the honeycomb to the sunflower structure when guest coronene is introduced. From MM simulations, it reveals that after co-assembled with coronene the total adsorption energy for the assembly of both BIC-C8 and BIC-C16 is increased, which contributes to the structural transition (Table S2).

**Table S2.** Simulated adsorption energies in multiple assemblies. The simulated results indicate the energies per unit area and are presented in kcal·mol<sup>-1</sup>·nm<sup>-2</sup>.

	BIC-C8 Honeycomb Structure	BIC-C8 Sunflower Structure I	BIC-C16 Honeycomb Structure	BIC-C16 Sunflower Structure II
Adsorption energy	-28.55	-30.60	-20.95	-21.35

## REFERENCE

1. J. R. Gong, S. B. Lei, L. J. Wan, G. J. Deng, Q. H. Fan and C. L. Bai, *Chem. Mater.*, 2003, **15**, 3098-3104.
2. C. E. Kundrot, J. W. Ponder and F. M. Richards, *J. Comput. Chem.*, 1991, **12**, 402-409.
3. T. A. Halgren, *J. Comput. Chem.*, 1996, **17**, 490-519.
4. P. Ren, C. Wu and J. W. Ponder, *J. Chem. Theory Comput.*, 2011, **7**, 3143-3161.
5. C.-A. Palma, M. Bonini, A. Llanes-Pallas, T. Breiner, M. Prato, D. Bonifazi and P. Samori, *Chem.*

*Commun.*, 2008, 5289-5291.